The Computational Fundamentals of Spatial Cycloidal Gearing

Giorgio Figliolini, Hellmuth Stachel and Jorge Angeles

Abstract The tooth flanks of bevel gears with involute teeth are still cut using approximations such as Tredgold's and octoid curves, while the geometry of the exact spherical involute is well known. The modeling of the tooth flanks of gears with skew axes, however, still represents a challenge to geometers. Hence, there is a need to develop algorithms for the geometric modeling of these gears. As a matter of fact, the modeling of gears with skew axes and involute teeth is still an open question, as it is not even known whether it makes sense to speak of such tooth geometries. This paper is a contribution along these lines, as pertaining to gears with skew axes and cycloid teeth. To this end, the authors follow and extend results reported by Martin Disteli at the turn of the 20th century concerning the general synthesis of gears with skew axes. The main goal is to shed light on the geometry of the tooth flanks of gears with skew axes. The dualization of the tooth profiles of spherical cycloidal gears leads to ruled surfaces as conjugate tooth flanks such that at any instant the contact points are located on a straight line. A main result reported herein is Theorem 5, which is original. All results are proven by means of a consistent use of dual vectors representing directed lines and rigid-body twists.

Giorgio Figliolini
Dipartimento di Meccanica, Stutture, Ambiente e Territorio, Università degli Studi di Cassino, Via Di Biasio 43, 03043 Cassino (Fr), Italy, e-mail: figliolini@unicas.it

Hellmuth Stachel
Institute of Discrete Mathematics and Geometry, Vienna University of Technology, Wiedner Hauptstr. 8-10/104, A 1040 Wien, Austria, e-mail: stachel@dmg.tuwien.ac.at

Jorge Angeles
Department of Mechanical Engineering & CIM, McGill University, 817 Sherbrooke Street West, Montréal (Québec), H3A 2K6, Canada, e-mail: angeles@cim.mcgill.ca

1 Introduction

While gear manufacturing is well developed, with precision gears cut under tight tolerances and producing smooth motions, the geometry of gear meshing is not yet fully exploited in the industry. For example, bevel gears are still designed using Tredgold's approximation, under which the tooth profile is designed so as to yield a projection onto the tangent plane of the *back cone* that matches the profile of an equivalent involute spur gear. Moreover, the teeth of straight bevel gears are cut following a second approximation, that is "convenient" in light of the shape of the cutting rack, which produces an *octoid*, namely, a curve on the surface of a sphere whose shape resembles a number eight. The octoid and the Tredgold-approximated involute are coincident only locally, around the pitch point of the latter, but differ away from this point. Not only this, involute profiles for gear pairs with skew axes have only appeared in the open literature as recently as six years ago, with the publication of Phillips' book [1]. However, Phillips' gear profiles rely on the assumption that the contact between teeth of meshing gears is punctual, which is too limiting. It is thus apparent that there is still substantial room for improvement in an otherwise highly developed technology. The aim of this paper is to lay down the fundamental concepts and the computational relations for the production of meshing gears with cycloid teeth and skew axes, as a means to pave the way toward the synthesis of gears with involute teeth and skew axes, if these are possible at all, which is, as yet, an open question.

We surmise here that gear-tooth contact can take place along lines. Within this paradigm, the computational fundamentals for the production of the tooth flanks of spatial gears with cycloid teeth are laid down in this paper. The approach relies on the dualization of the tooth profiles of spherical cycloidal gears, which are briefly recalled here, and which are based on the seminal work of Martin Disteli, as reported by the authors [2]. In fact, Disteli transferred Reuleaux's principle of gearing ([3, p. 143]) for the particular case of cycloidal gears from the sphere into 3D space [4, 5]. This led to the synthesis of meshing skew gears whose tooth flanks are ruled surfaces in contact along straight lines.

Proposed here is a procedure to synthesize the tooth profiles of meshing gears with *cycloid* teeth, as a first attempt to the synthesis of tooth profiles with involute shapes. The procedure is described below: 1) the *hyperboloid* pitch surfaces that are derived from the relative layout between the two skew axes and the constant transmission ratio are first obtained; 2) the cylindroid determined by the relative motion of the two meshing gears, for a given transmission ratio, is then synthesized as the locus of the *instant screw axis* (ISA); 3) with the aid of the cylindroid, we introduce an *auxiliary surface* (AS); and 4) as the AS moves while maintaining *line contact* with the two hyperboloid pitch surfaces, a pair of conjugate flanks is synthesized. The AS is a *cylinder* in the case of spur cycloidal gears, a *cone* in the case of bevel cycloidal gears, and a *helical surface* in the case of skew cycloidal gears, as we show in this paper.

We have thus extended Franz Reulaux's approach to the case of skew cycloidal gears. This approach could be extended further, to the case of involute skew gears, but the extension is challenging because each tooth flank should be obtained as the envelope of a given surface attached to the AS.

2 The Fundamentals of Cycloidal Gearing

We start by recalling Reuleaux's principle in the planar case, which sometimes is attributed to Ch. E. L. Camus (1733). However, we focus on a point of view which opens the way for a transfer to the spatial version:

Let Σ_2, Σ_3 be frames attached to the two wheels of spur gears with centers O_2, O_3, respectively, mounted on the machine frame Σ_1. The pitch circles of the gears are denoted by p_2 and p_3. Then, Reuleaux's principle states:

Theorem 1 *If an auxiliary curve p_4 rolls on the pitch circles p_2 and p_3, then any point C attached to p_4 traces conjugate profiles c_2 and c_3, fixed to p_2 and p_3, respectively.*

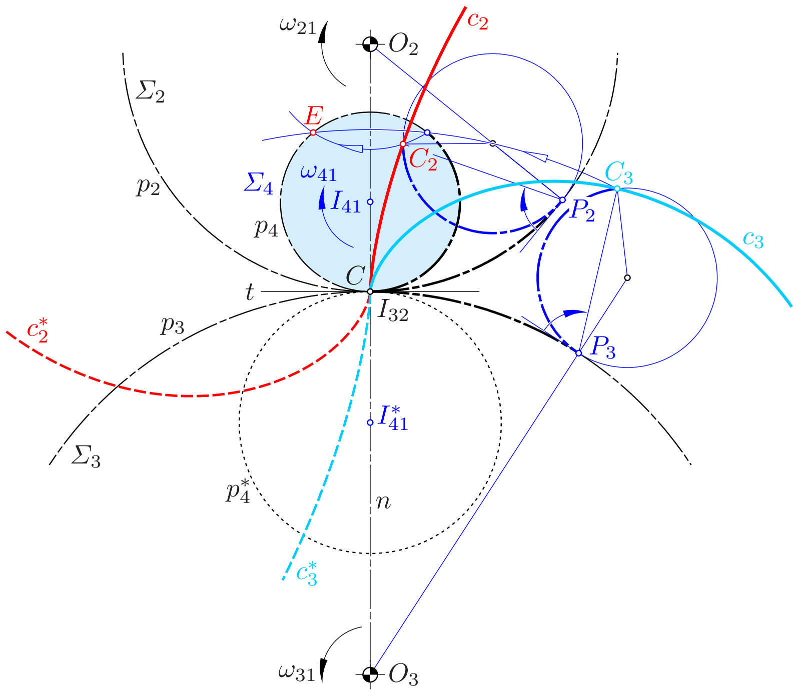

Fig. 1 Reuleaux's principle in the plane

In the special case of *cycloidal gearing*, p_4 is a circle and the point C attached to p_4 happens to be located on p_4, as depicted in Fig. 1.

Now we rephrase Theorem 1 by introducing an additional frame Σ_4, which contains the auxiliary curve p_4:

> Suppose that simultaneously with the two wheels Σ_2, Σ_3 rotating about their centers O_2, O_3, the auxiliary frame Σ_4 moves with respect to the machine frame Σ_1 such that the auxiliary curve p_4 rolls on p_2, p_3, and contact takes place at the same point $I_{42} = I_{43} = I_{32}$ fixed in Σ_1. Then, if C is any point attached to Σ_4 and different from the instant center $I_{42} = I_{43}$, the relative paths c_2, c_3 of C under Σ_4/Σ_2 and Σ_4/Σ_3, respectively, are in contact at C, since the respective normals pass through $I_{42} = I_{43}$. Hence, $c_2 \subset \Sigma_2$ and $c_3 \subset \Sigma_3$ are conjugate tooth profiles of Σ_3/Σ_2.

Remarks:

1. Reuleaux's principle is also valid in the spherical case, i.e., for bevel gears.
2. This principle can be generalized in the following way: Instead of a point $C \in \Sigma_4$ a smooth curve $c_4 \subset \Sigma_4$ can be given. Then the *envelopes* c_2, c_3 of c_4 under Σ_4/Σ_2 and Σ_4/Σ_3, respectively, are conjugate tooth flanks, and the envelope c_1 of c_4 under Σ_4/Σ_1 is the contact line.

3 Reulaux's Principle for Skew Gears

Let the motions of two gears be given, i.e., the rotations Σ_2/Σ_1, Σ_3/Σ_1 about fixed skew axes p_{10} and p_{20} with angular velocities ω_{10}, ω_{20}, respectively. In analogy to the planar case we ask:

Question: *Is there an "auxiliary frame" Σ_4 which can move in such a way that the motions Σ_4/Σ_2 and Σ_4/Σ_3 have twists with the same axis p_{32} and the same pitch $h_{32} = \omega_{320}/\omega_{32}$ as the relative motion Σ_3/Σ_2 of the two gears?*

We translate this into dual vector notation (see, e.g., [6, 7]) using the standard nomenclature: ω_{ij} denotes the angular velocity and ω_{ij0} the translatory velocity of the relative motion Σ_i/Σ_j; both velocities are combined in the *dual velocity* $\widehat{\omega}_{ij} = \omega_{ij} + \varepsilon\omega_{ij0}$, with ε denoting the *dual unit*, defined as $\varepsilon \neq 0$, $\varepsilon^2 = 0$. The instant axis p_{ij} is described by the *dual unit vector* $\widehat{\boldsymbol{p}}_{ij} = \boldsymbol{p}_{ij} + \varepsilon\boldsymbol{p}_{ij0}$. The instant *twist* of Σ_i/Σ_j reads

$$\widehat{\boldsymbol{q}}_{ij} = \widehat{\omega}_{ij}\,\widehat{\boldsymbol{p}}_{ij} = (\omega_{ij} + \varepsilon\omega_{ij0})(\boldsymbol{p}_{ij} + \varepsilon\boldsymbol{p}_{ij0}).$$

From the given wheels we have

$$\widehat{\boldsymbol{q}}_{21} = \omega_{21}\widehat{\boldsymbol{p}}_{21} \quad \text{and} \quad \widehat{\boldsymbol{q}}_{31} = \omega_{31}\widehat{\boldsymbol{p}}_{31} \quad \text{with} \quad \omega_{21}, \omega_{31} \in \mathbb{R}.$$

According to the foregoing question we seek a frame Σ_4 such that

$$\widehat{\boldsymbol{p}}_{42} = \widehat{\boldsymbol{p}}_{43} = \widehat{\boldsymbol{p}}_{32}$$

and the corresponding *dual velocities* are proportional, i.e., there are real coefficients $\lambda_2, \lambda_3 \in \mathbb{R}$ such that

$$\widehat{\omega}_{42} = \lambda_2 \, \widehat{\omega}_{32} \text{ and } \widehat{\omega}_{43} = \lambda_3 \, \widehat{\omega}_{32}.$$

This implies

$$\widehat{\boldsymbol{q}}_{42} = \lambda_2 \, \widehat{\boldsymbol{q}}_{32} \text{ and } \widehat{\boldsymbol{q}}_{43} = \lambda_3 \, \widehat{\boldsymbol{q}}_{32} \text{ for } \lambda_2, \lambda_3 \in \mathbb{R}.$$

Due to the Aronhold-Kennedy theorem [8] we obtain

$$\widehat{\boldsymbol{q}}_{41} - \widehat{\boldsymbol{q}}_{21} = \lambda_2(\widehat{\boldsymbol{q}}_{31} - \widehat{\boldsymbol{q}}_{21}) \text{ and } \widehat{\boldsymbol{q}}_{41} - \widehat{\boldsymbol{q}}_{31} = \lambda_3(\widehat{\boldsymbol{q}}_{31} - \widehat{\boldsymbol{q}}_{21}).$$

Hence, $\widehat{\boldsymbol{q}}_{41}$ can be expressed in two ways as a real linear combination of $\widehat{\boldsymbol{q}}_{21}$ and $\widehat{\boldsymbol{q}}_{31}$:

$$\widehat{\boldsymbol{q}}_{41} = \lambda_2 \, \widehat{\boldsymbol{q}}_{31} + (1-\lambda_2)\widehat{\boldsymbol{q}}_{21} = (1+\lambda_3)\widehat{\boldsymbol{q}}_{31} - \lambda_3 \, \widehat{\boldsymbol{q}}_{21} \tag{1}$$

$$\widehat{\boldsymbol{q}}_{41} = \lambda_2 \, \omega_{31}\widehat{\boldsymbol{p}}_{31} + (1-\lambda_2)\omega_{21}\widehat{\boldsymbol{p}}_{21} = (1+\lambda_3)\omega_{31}\widehat{\boldsymbol{p}}_{31} - \lambda_3 \, \omega_{21}\widehat{\boldsymbol{p}}_{21}. \tag{2}$$

As long as the gear axes p_{21} and p_{31} are different, the dual unit vectors $\widehat{\boldsymbol{p}}_{21}$ and $\widehat{\boldsymbol{p}}_{31}$ are linearly independent as well as their real multiples $\widehat{\boldsymbol{q}}_{21} = \omega_{21}\widehat{\boldsymbol{p}}_{21}$ and $\widehat{\boldsymbol{q}}_{31} = \omega_{31}\widehat{\boldsymbol{p}}_{31}$. We thus may compare coefficients in eq.(1): Both equations can be simultaneously satisfied by setting

$$\lambda_3 = \lambda_2 - 1. \tag{3}$$

Equation (1) then reveals that the twist $\widehat{\boldsymbol{q}}_{41}$ is a real linear combination of the twists $\widehat{\boldsymbol{q}}_{21}$ and $\widehat{\boldsymbol{q}}_{31}$. Hence, $\widehat{\boldsymbol{q}}_{41}$ is the twist of the relative motion between two 'virtual' gears with axes p_{21} and p_{31} when, by virtue of eq.(2), the corresponding angular velocities $\nu_{31} : \nu_{21}$ obey

$$\nu_{31} : \nu_{21} = \lambda_2 \, \omega_{31} : (\lambda_2 - 1)\omega_{21} = (1+\lambda_3)\omega_{31} : \lambda_3 \, \omega_{21}. \tag{4}$$

Due to results of Plücker and Ball the instant axis p_{41} of the motion Σ_4/Σ_1, i.e., of the auxiliary frame with respect to the machine frame, is located on the Plücker conoid Ψ ([2, Fig. 6]) defined by the given gear axes p_{21} and p_{31}.

This is not only necessary, but also sufficient, because, conversely, any transmission ratio $\nu_{31} : \nu_{21}$ gives, by virtue of eq.(4),

$$\lambda_2 = \omega_{21}\nu_{31}/(\nu_{21}\omega_{31} - \nu_{31}\omega_{21}),$$

provided that $\nu_{31} : \nu_{21} \neq \omega_{31} : \omega_{21}$. Otherwise, the twist $\widehat{\boldsymbol{q}}_{41}$ would be a real multiple of $\widehat{\boldsymbol{q}}_{32} = \omega_{31}\widehat{\boldsymbol{p}}_{31} - \omega_{21}\widehat{\boldsymbol{p}}_{21}$, and hence, $p_{41} = p_{32}$.

For a detailed analysis we use a Cartesian coordinate frame $\mathcal{F}(O; x_1, x_2, x_3)$ with $\widehat{\boldsymbol{e}}_1, \widehat{\boldsymbol{e}}_2$ denoting the dual unit vectors of the x_1- and x_2-axes. The given axes p_{21} and p_{31} of the wheels are assumed to be symmetrically placed with respect to the x_1- and x_2-axes, as depicted in Fig. 2. Therefore, using the *dual angle* $\widehat{\alpha} = \alpha + \varepsilon\alpha_0$, we can set up

$$\begin{aligned} \widehat{\boldsymbol{p}}_{21} &= \widehat{\boldsymbol{e}}_1 \cos\widehat{\alpha} - \widehat{\boldsymbol{e}}_2 \sin\widehat{\alpha} \\ \widehat{\boldsymbol{p}}_{31} &= \widehat{\boldsymbol{e}}_1 \cos\widehat{\alpha} + \widehat{\boldsymbol{e}}_2 \sin\widehat{\alpha}\,. \end{aligned} \tag{5}$$

We limit ourselves to the skew case and assume

$$0 < \alpha < \pi/2 \ \text{ and } \ \ \alpha_0 \neq 0 \tag{6}$$

though all arguments hold also in the spherical case, $\alpha_0 = 0$, and in the planar case, $\alpha = 0$, with parallel axes.

In addition, we denote the dual angle between the relative axes $\widehat{\boldsymbol{p}}_{32}$ and $\widehat{\boldsymbol{e}}_1$ by $\widehat{\varphi}$ and that between the generator $\widehat{\boldsymbol{p}}_{41}$ and $\widehat{\boldsymbol{e}}_1$ by $\widehat{\beta}$ (Fig. 2). We can thus set up

$$\begin{aligned} \widehat{\boldsymbol{p}}_{32} &= \widehat{\boldsymbol{e}}_1 \cos\widehat{\varphi} + \widehat{\boldsymbol{e}}_2 \sin\widehat{\varphi} \\ \widehat{\boldsymbol{p}}_{41} &= \widehat{\boldsymbol{e}}_1 \cos\widehat{\beta} + \widehat{\boldsymbol{e}}_2 \sin\widehat{\beta}\,. \end{aligned} \tag{7}$$

As the instant screw axis (ISA) p_{32} and the line p_{41} are located on the Plücker conoid Ψ, we derive from eqs. [2, (10), (11)]

$$\varphi_0 = R\sin 2\varphi \ \text{ and } \ \ \beta_0 = R\sin 2\beta \ \text{ with } \ \ R = \frac{\alpha_0}{\sin 2\alpha} \tag{8}$$

and from eq.[2, (15)],

$$h_{32} = \frac{\omega_{320}}{\omega_{32}} = R(\cos 2\alpha - \cos 2\varphi), \quad h_{41} = \frac{\omega_{410}}{\omega_{41}} = R(\cos 2\alpha - \cos 2\beta). \tag{9}$$

All this can be visualized in the Ball-Disteli diagram—cf. [2, Fig. 5].

We summarize:

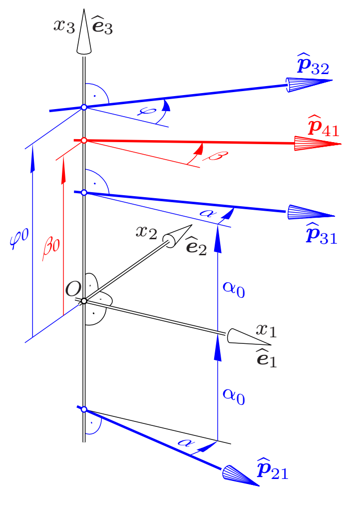

Fig. 2 Axes $\widehat{\boldsymbol{p}}_{21}$, $\widehat{\boldsymbol{p}}_{31}$ of the gear wheels, the ISA $\widehat{\boldsymbol{p}}_{32}$ and the axis $\widehat{\boldsymbol{p}}_{41}$ of the auxiliary system Σ_4

Theorem 2 (Disteli, [5])
For given wheels Σ_2, Σ_3 with fixed skew axes p_{21}, p_{31} and angular velocities ω_{21}, ω_{31}, there is an auxiliary frame Σ_4 such that the screws of Σ_4/Σ_2, Σ_4/Σ_3 and Σ_3/Σ_2 are equal at every instant if and only if the instant axis p_{41} of Σ_4/Σ_1 is located on the Plücker conoid Ψ, but different from p_{32}, and the instant pitch $h_{41} = \omega_{410}/\omega_{41}$ is defined by eq.(9).

Due to Theorem 2, we can proceed on Martin Disteli's approach to generalizing the planar or spherical cycloidal gearing to the spatial analogue stated in Theorem 3:

We keep the axis p_{41} of Σ_4/Σ_1 fixed in the machine frame and move simultaneously Σ_2 with the twist $\widehat{\boldsymbol{q}}_{21}$ and Σ_3 with the twist $\widehat{\boldsymbol{q}}_{31}$. Furthermore, we move Σ_4 about the axis p_{41} with pitch h_{41} such that according to Theorem 2 the relative axes p_{42} and p_{43} coincide permanently with p_{32}—the corresponding angular velocity ω_{41} will be determined in Section 4.

Under these motions the axodes of the relative motions Σ_3/Σ_2, Σ_4/Σ_2 and Σ_4/Σ_3 are obtained by applying the inverse motions Σ_1/Σ_2, Σ_1/Σ_3 and Σ_1/Σ_4 to the relative axis p_{32}, which is fixed to Σ_1. This means in detail: The rotations Σ_2/Σ_1 and Σ_3/Σ_1 about the gear axes p_{21} and p_{31} generate one-sheet hyperboloids $\Pi_2 \subset \Sigma_2$ and $\Pi_3 \subset \Sigma_3$, respectively. These are the axodes of the relative motion Σ_3/Σ_2 between the gears. Under the helical motion with pitch h_{41} about p_{41} the relative axis p_{32} sweeps a helical surface Π_4, which, together with Π_2, forms the axodes of Σ_4/Σ_2. In the same way Π_3 and Π_4 are the axodes of Σ_4/Σ_3. Obviously, Π_2, Π_3 and Π_4 are the spatial analogues of the circles p_2, p_3 and p_4 in Fig. 1. The spatial analogue to the pole normal n, the locus of the auxiliary center I_{41}, is the Plücker conoid Ψ as the locus of possible auxiliary axes p_{41} [9].

It is necessary to choose p_{41} different from p_{21} and p_{31}, because, e.g., $p_{41} = p_{21}$ implies $\Sigma_4 = \Sigma_2$; the relative motion Σ_4/Σ_2 has a permanent standstill with indeterminate pitch $0/0$. Therefore, this is only a trivial solution of the question asked above and answered in Theorem 2. The case $p_{41} = p_{32}$ is impossible by (4).

Theorem 3 *Let p_{41} be any specified generator of the Plücker conoid Ψ, but different from p_{21}, p_{31}, p_{32}. Let Π_4 be the ruled helical surface traced by the relative axis p_{32} under the helical motion about p_{41} with pitch h_{41}. Then the motions Σ_4/Σ_2 and Σ_4/Σ_3 are defined by the rolling and sliding of Π_4 with the hyperboloids Π_2, Π_3, respectively.*
For any line g attached to Σ_4 the surfaces Φ_2, Φ_3 traced by g under the relative motions Σ_4/Σ_2 and Σ_4/Σ_3, respectively, are conjugate tooth flanks of Σ_3/Σ_2.
For these flanks at any instant the meshing points are located on a straight line. In the machine frame Σ_1 the locus of these lines, i.e., the meshing surface, is traced by g under Σ_4/Σ_1 with the fixed twist $\widehat{\boldsymbol{q}}_{41} = \omega_{41}(1 + \varepsilon h_{41})\widehat{\boldsymbol{p}}_{41}$. Hence, the meshing surface is a ruled helical surface, too.

Proof. For any given tooth flank Φ_3 attached to Σ_3 a point $C \in \Phi_3$ is instantly a meshing point if its velocity vector $\boldsymbol{v}_{32}$ under Σ_3/Σ_2 is tangent to Φ_3.

Now let us focus on any posture where the three axodes are in mutual contact along p_{32}. Wherever line g is chosen in space, for any point $C \in g$ the velocity vectors $\boldsymbol{v}_{32}$ under Σ_3/Σ_2, $\boldsymbol{v}_{42}$ under Σ_4/Σ_2 and $\boldsymbol{v}_{43}$ under Σ_4/Σ_3 are proportional, as the screws are identical. Hereby vector $\boldsymbol{v}_{43}$ is tangent to the surface Φ_3 swept by g under Σ_4/Σ_3. Hence, C is a point of contact between Φ_3 and its conjugate tooth flank in Σ_2, which is the envelope of Φ_3 under the relative motion Σ_3/Σ_2.

Under Σ_4/Σ_2 line g sweeps the surface Φ_2. In the given posture the tangent planes of Φ_2 and Φ_3 have the line g in common and at each point $C \in g$ also the line spanned by the velocity vector $\boldsymbol{v}_{32}$. So, the two surfaces share their tangent plane at C. There is just one exception: When $\boldsymbol{v}_{32}$ has the direction of g, then there is no unique plane spanned. However, in this exceptional case g is torsal on Φ_2 and Φ_3, while C is the common cuspidal point of this generator. Moreover, by definition, such a singularity of Φ_3 is always part of its envelope under Σ_3/Σ_2. Hence, in any case Φ_2 is conjugate to Φ_3. The postures considered of these surfaces are in contact at all points of the straight line g (see Fig. 3).

4 Spatial Cycloidal Gearing

As an analogue to the planar case displayed in Fig. 1 we keep $p_{41} \in \Psi$ fixed and start with the generator $g = p_{32}$. Then, the tooth flanks Φ_2 and Φ_3 are dualized spherical trochoids, as g is attached to Σ_4 while the ruled helical surface $\Pi_4 \subset \Sigma_4$ rolls and slides on Π_2 and Π_3, respectively. Figure 3 shows the conjugate flanks Φ_2 and Φ_3 in a general pose.

Rolling and sliding (German: schroten) of Π_4 along Π_2 means that at each instant Π_4 contacts Π_2 along a common generator. Therefore, the respective Frenet frames coincide. Moreover, the director cones of the two axodes roll on each other. The *director cone* of any ruled surface is obtained by drawing the parallel line to each generator through the origin. The director cones of Π_2, Π_3 and Π_4 are all cones of revolution.

By applying the *dual sine theorem* to the triplet of frames $(\Sigma_1, \Sigma_2, \Sigma_4)$ with respective twists $\widehat{\omega}_{41}\widehat{\boldsymbol{p}}_{41} - \omega_{21}\widehat{\boldsymbol{p}}_{21} = \widehat{\omega}_{42}\,\widehat{\boldsymbol{p}}_{32}$ we obtain

$$\frac{\widehat{\omega}_{21}}{\sin(\widehat{\varphi} - \widehat{\beta})} = \frac{\widehat{\omega}_{41}}{\sin(\widehat{\varphi} + \widehat{\alpha})} = \frac{\widehat{\omega}_{42}}{\sin(\widehat{\alpha} + \widehat{\beta})}. \tag{10}$$

In particular, the primal part of

$$\widehat{\omega}_{21}\,\sin(\widehat{\varphi} + \widehat{\alpha}) = \widehat{\omega}_{41}\,\sin(\widehat{\varphi} - \widehat{\beta})$$

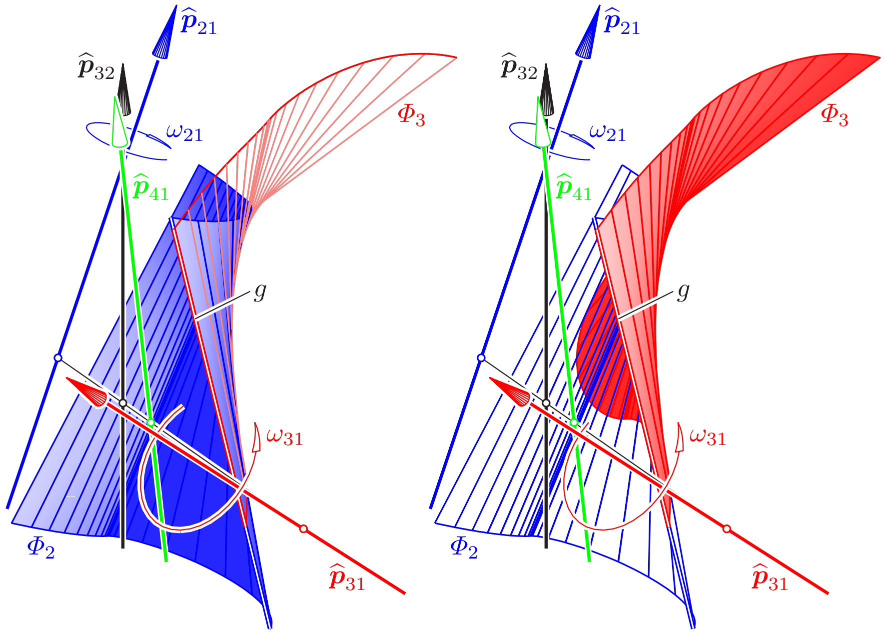

Fig. 3 Conjugate tooth flanks Φ_2, Φ_3 in contact along line g in the case $\alpha = 35°$, $\alpha_0 = 40.0$, $\omega_{31} : \omega_{21} = -1 : 2$, $\varphi - \beta = 6.5°$.

expresses the rolling of the director cones of Π_2 and Π_4. Furthermore, we specialize Theorem 3 below:

Corollary 4 *For spatial cycloidal gearing the tooth flank Φ_2 is the trace of line $g = p_{32}$ under the motion Σ_4/Σ_2, i.e., under the composition of the helical motion Σ_4/Σ_1 about p_{41} with angular velocity*

$$\omega_{41} = \frac{\omega_{21}\,\sin(\varphi + \alpha)}{\sin(\varphi - \beta)}$$

and pitch h_{41}, given by eq.(9), and the rotation Σ_1/Σ_2 about p_{21} with angular velocity $-\omega_{21}$. The conjugate flank Φ_3 is the trace of line $g = p_{32}$ under the composition Σ_4/Σ_3 of the helical motion Σ_4/Σ_1 and the rotation Σ_1/Σ_3 about p_{31} with angular velocity $-\omega_{31}$.

We conclude with an original result, namely, the spatial analogue of the generalized Reuleaux principle noted in Remark 2 above.

Theorem 5 *Let the motions Σ_4/Σ_2 and Σ_4/Σ_3 be defined like in Theorem 3. Then, for any smooth surface Γ attached to Σ_4 the envelopes Φ_2, Φ_3 of Γ under the relative motions Σ_4/Σ_2 and Σ_4/Σ_3, respectively, are conjugate tooth flanks of Σ_3/Σ_2.*

Sketch of a *proof*: Point C is a point of contact between Γ and its envelope Φ_2 under Σ_4/Σ_2 if and only if the surface normal $\widehat{\boldsymbol{n}}$ of Γ at C is included in the linear line complex with equation $\boldsymbol{q}_{420} \cdot \boldsymbol{n} + \boldsymbol{q}_{42} \cdot \boldsymbol{n}_0 = 0$. By Theorem 2 the twists $\widehat{\boldsymbol{q}}_{43}$ und $\widehat{\boldsymbol{q}}_{32}$ are real multiples of $\widehat{\boldsymbol{q}}_{42}$. Hence, the corresponding linear line complexes are equal, and C is at the same time an enveloping point for Σ_4/Σ_3.

5 Conclusions

The main goal of this paper is to shed light on the geometry of the tooth flanks of gears with skew axes. To this end, the authors follow and extend results reported by Martin Disteli, thereby deriving ruled surfaces as conjugate tooth flanks in contact along a line. The algebra of dual vectors representing directed lines and rigid-body twists proves to be an invaluable tool in this endeavor.

A detailed analysis of the tooth flanks thus obtained is left for future research. Theorem 5, a main result reported in this paper, should lead to optimum tooth flanks in the sense of minimizing the power losses caused by Coulomb friction upon sliding, which is unavoidable in gears with skew axes.

References

1. Phillips, J. (2003). *General Spatial Involute Gearing.* Springer Verlag, New York.
2. Figliolini, G., Stachel, H., Angeles, J. (2007). A New Look at the Ball-Disteli Diagram and Its Relevance to Spatial Gearing. *Mech. Mach. Theory* 42(10), 1362–1375.
3. Reuleaux, F. (1875). *Theoretische Kinematik I.* Verlag Friedrich Vieweg und Sohn, Braunschweig.
4. Disteli, M. (1904). Über instantane Schraubengeschwindigkeiten und die Verzahnung der Hyperboloidräder. *Z. Math. Phys.* 51, 51–88.
5. Disteli, M. (1911). Über die Verzahnung der Hyperboloidräder mit geradlinigem Eingriff, *Z. Math. Phys.* 59, 244–298.
6. Blaschke, W. (1960). *Kinematik und Quaternionen.* VEB Deutscher Verlag der Wissenschaften, Berlin.
7. Veldkamp, G. R. (1976). On the Use of Dual Numbers, Vectors, and Matrices in Instantaneous Spatial Kinematics. *Mech. and Mach. Theory* 11, 141–156.
8. Beggs, J.S. (1959). *Ein Beitrag zur Analyse räumlicher Mechanismen.* Dr.-Ing. Dissertation, Technische Hochschule Hannover, Hanover, Germany.
9. Figliolini, G., Angeles, J. (2006). The synthesis of the pitch surfaces of internal and external skew-gears and their racks. *ASME Journal of Mechanical Design* 128(4), 794–802.
10. Stachel, H. (2000). Instantaneous spatial kinematics and the invariants of the axodes. *Proc. Ball 2000 Symposium* (no. 23), Cambridge.
11. Müller, H. R. (1963). *Kinematik.* Sammlung Göschen, Walter de Gruyter & Co, Berlin.